



Unsteady MHD convection and mass transfer flow of micropolar fluids past a vertical permeable moving plate with heat absorption

Mohamed M Abdelkhalek

Department of Nuclear Physics, Nuclear Research Centre, Atomic Energy Authority,
Inshas, P.O. Box-13759, Cairo, Egypt

E-mail: Mohamed_moustafa_2000@yahoo.com

Received 1 December 2005, accepted 27 February 2006

Abstract : By the use of the theory of micropolar fluids due to Eringen, perturbation method is presented to study an unsteady MHD convection and mass transfer flow of micropolar fluids past a vertical permeable moving plate with heat absorption. The plate moves with a constant velocity in the direction of fluid flow, while the free stream velocity follows an exponentially increasing or decreasing small perturbation law. Approximate solutions of the coupled nonlinear governing equations are obtained for different values of microrotation and magnetic parameters. Numerical calculations are carried out for the various parameters entering into the problem. The results of velocity, angular velocity, temperature and concentration profiles have been presented graphically for various values of the material parameters. The results indicate that the micropolar fluids display a reduction in drag as well as heat transfer rate when compared with Newtonian fluids.

Keywords . Magnetohydrodynamic, heat and mass transfer, micropolar fluids

PACS Nos. . 44.25.+f, 44.05.+e, 47.27.Te

1. Introduction

The theory of micropolar fluids as developed by Eringen [1,2], which includes the effect of local rotary inertia, the couple stresses and inertial spin satisfactorily provides a model for the non-Newtonian behavior observed in the polymers, paints, lubricants, suspended fluids and blood *etc.* Eringen [3] also developed the theory of micropolar fluids for the case where only microrotational inertia exists. He extended the theory of thermomicropolar fluids and derived the constitutive laws for fluids with microstructure. Simple problems on the flow of such fluids were studied by a number of researchers and a review of this work was given by Ariman and Turk and Sylvester [4]. The equations governing the flow of a micropolar fluid involve a microrotation vector and a gyration parameter in addition to the classical velocity vector field. This theory may be applied to explain the flow of colloidal solutions, liquid crystals, fluids, with additives, suspension solutions, animal blood, and many other situations. Also, the continuous surface concept was introduced by Sakiadis [5]. Continuous surfaces are surfaces such as those of polymers sheets or filaments continuously drawn from a die. The boundary layer flow on continuous

surfaces is an important type of flow occurring in a number of technical processes. Examples may be found in continuous casting, glass fiber production, metal extrusion, hot rolling, the cooling and or drying of paper and textiles, and wire drawing [6,8]. The study of heat transfer and the flow field is necessary for determining the quality of the final products of these processes as explained by Karwe and Jaluria [9]. The extension of above type of flows to include MHD effects has become important due to several engineering applications such as in MHD generators, designing cooling system for nuclear reactors, flow meters, *etc.* where the micro concentration provides an important parameter for deciding the rate of heat flow. By simulating it, one can obtain the desired temperature in such equipments. Several investigators have made theoretical and experimental studies of micropolar flow in the presence of a transverse magnetic field during the last three decades. Magnetohydrodynamic heat transfer can be divided into two sections: in the first section, the electromagnetic fields are used to control the heat transfer as in the convection flows and aerodynamic heating, while in the second section, the heating is produced by the electromagnetic fields as in such MHD

devices as generators, pumps, *etc.* Gorla [10] investigated the forced convective heat transfer in a micropolar boundary layer flow on a vertical flat plate. Mahammadein and Gorla [11] analyzed the effects of magnetic field on the laminar boundary mixed convection flow of a micropolar fluid over a horizontal plate. Takhar and Soundalgekar [12] studied the effects of suction and injection on the flow of a micropolar fluid past a continuously moving semi-infinite porous plate. The natural convection flow of micropolar fluids in a porous medium was studied by Mahammadein and Mansour [13]. El-Hakeim [14] analyzed the effects of magnetic field of natural convection with temperature-dependent viscosity in micropolar fluids. The same author [15] studied the effects of a transverse magnetic field on the natural convection boundary layer flow of micropolar fluids in porous media. Effects of Joule heating on the magnetohydrodynamic-free convection flow of a micropolar fluid were studied by El-Hakiem *et al* [16].

In the present study, we have analyzed the problem of unsteady MHD convection and mass transfer flow of polar fluids past a vertical permeable moving plate with heat absorption. The governing differential equations have been solved by using the perturbation technique. The velocity, microrotation, concentration and temperature functions are shown graphically and the effects of magnetic field, micropolar, and heat absorption parameters are studied.

2. Mathematical formulation

Let us consider a two-dimensional, unsteady flow of a laminar, incompressible, viscous, electrically conducting and heat absorbing micropolar fluid past a semi-infinite, vertical porous moving plate embedded in a porous medium and subjected to a transverse magnetic field in the presence of thermal and concentration buoyancy effects. It is assumed that there is no applied voltage, which implies the absence of an electrical field. The transversely applied magnetic field and magnetic Reynolds number are very small and hence, the induced magnetic field is negligible [17]. Viscous and Darcy's resistance terms are taken into account with constant permeability of the porous medium. The MHD term is derived from an order of magnitude analysis of the full Navier-Stokes equations. It is assumed here that the hole size of the porous plate is significantly larger than a characteristic microscopic length scale of the porous medium. We regard the porous medium as an assemblage of small identical spherical particles fixed in space, following Yamamoto and Iwamura [18]. The governing equations for this investigation are based on the balances of mass, linear momentum, angular momentum energy and concentration species. Taking into consideration the assumptions made above, these equations can be written as follows:

$$\frac{\partial \bar{v}}{\partial \bar{y}} = 0, \quad (1)$$

$$\frac{\partial \bar{u}}{\partial \bar{t}} + \bar{v} \frac{\partial \bar{u}}{\partial \bar{y}} = -\frac{1}{\rho} \frac{\partial \bar{P}}{\partial \bar{x}} + (v + v_r) \frac{\partial^2 \bar{u}}{\partial \bar{y}^2} + g\beta_T(T - T_\infty) + g\beta_C(C - C_\infty) - v \frac{\bar{u}}{K} - \frac{\delta}{\rho} B_0^2 \bar{u} + 2v_r \frac{\partial \bar{\omega}}{\partial \bar{y}}, \quad (2)$$

$$\rho \bar{j} \left(\frac{\partial \bar{\omega}}{\partial \bar{x}} + \bar{v} \frac{\partial \bar{\omega}}{\partial \bar{y}} \right) = \gamma \frac{\partial^2 \bar{\omega}}{\partial \bar{y}^2}, \quad (3)$$

$$\frac{\partial T}{\partial \bar{t}} + \bar{v} \frac{\partial T}{\partial \bar{y}} = \alpha \frac{\partial^2 T}{\partial \bar{y}^2} - \frac{Q_0}{\rho C_p} (T - T_\infty), \quad (4)$$

$$\frac{\partial C}{\partial \bar{t}} + \bar{v} \frac{\partial C}{\partial \bar{y}} = D \frac{\partial^2 C}{\partial \bar{y}^2} \quad (5)$$

In the previous equations, \bar{u}, \bar{v} - being the velocity components in the \bar{x}, \bar{y} - directions, respectively, g - is the acceleration due to gravity, β_T - the coefficient of volume expansion, β_C - the volumetric coefficient of expansion with concentration, T and T_∞ - the temperature of the fluid inside the thermal boundary layer and in the free stream, respectively, ρ - the fluid density, ν - the kinematics viscosity, C_p - the specific heat at constant pressure, σ - the fluid electrical conductivity, \bar{K} - the permeability of the porous medium, Q_0 - the dimensional heat absorption coefficient, C - the dimensional concentration, α - the fluid thermal diffusivity, D - the chemical molecular diffusivity, γ - the spin gradient viscosity, \bar{j} - the micro-inertia density, $\bar{\omega}$ - the component of the angular velocity vector normal to the xy - plane, v_r - the kinematics rotational viscosity. The third term on the RHS of momentum equation (2) denotes thermal buoyancy effects, the fourth is the concentration buoyancy effects, the fifth is the bulk matrix linear resistance, *i.e.* Darcy term, and the sixth is the MHD term. The magnetic and viscous dissipations are neglected. Also, the last term of the energy equation (4) represents the heat absorption effects. It is assumed that the porous plate moves with constant velocity \bar{u}_p in the longitudinal direction and the free stream velocity \bar{U}_∞ follows an exponentially increasing or decreasing small perturbation law. We also assume that the plate temperature T and suction velocity \bar{v} and the concentration on the plate vary exponentially with time. Under these assumptions, the appropriate boundary conditions for the velocity, temperature and concentration fields are

$$\bar{u} = \bar{u}_p, \quad T = T_w + \varepsilon(T_w - T_\infty)e^{\bar{n}\bar{t}}, \quad C = C_w + \varepsilon(C_w - C_\infty)e^{\bar{n}\bar{t}}, \quad \frac{\partial \bar{\omega}}{\partial \bar{y}} = -\frac{\partial^2 \bar{u}}{\partial \bar{y}^2} \text{ at } \bar{y} = 0, \quad (6)$$

$$u \rightarrow U_\infty = U_0(1 + \varepsilon e^{\bar{t}i}), \quad T \rightarrow T_\infty,$$

$$C \rightarrow C_\infty, \quad \bar{\omega} \rightarrow 0 \quad \text{as } \bar{y} \rightarrow \infty, \quad (7)$$

where, C_w and T_w - are the wall dimensional concentration and temperature, respectively. C_∞ and T_∞ - are the free stream dimensional concentration and temperature respectively. U_0 and \bar{n} - are constants.

From the continuity eq. (1), it is clear that the suction velocity normal to the plate is a function of time only. Assuming that it takes the following exponential form

$$\bar{v} = -V_0(1 + \varepsilon A e^{\bar{t}i}), \quad (8)$$

where, A is a real positive constant, ε and εA are small less than unity, and V_0 is a scale of suction velocity which has non-zero positive constant. Outside the boundary layer, eq. (2) gives

$$-\frac{1}{\rho} \frac{d\bar{P}}{d\bar{x}} = \frac{d\bar{U}_\infty}{d\bar{t}} + \frac{\nu}{K} \bar{U}_\infty + \frac{\sigma}{\rho} B_0^2 \bar{U}_\infty. \quad (9)$$

We now introduce the dimensionless variables as follows:

$$\bar{u} = U_0 u, \quad \bar{v} = V_0 v, \quad yv = V_0 \bar{y}, \quad U_\infty = U_0 U_\infty,$$

$$\bar{\omega} = \frac{U_0 V_0 \omega}{\nu}, \quad \bar{t} V_0 = t v, \quad M = \frac{\sigma B_0^2 \nu}{\rho V_0^2}, \quad \bar{u}_p = U_0 U_p,$$

$$\theta = \frac{T - T_\infty}{T_w - T_\infty}, \quad C = \frac{C - C_\infty}{C_w - C_\infty}, \quad \phi = \frac{\nu Q_0}{\rho C_p V_0^2},$$

$$\bar{K} V_0^2 = K v^2, \quad \bar{j} V_0^2 = j v^2, \quad P_r = \frac{\nu}{\alpha}, \quad S_c = \frac{\nu}{D}, \quad \bar{n} v = n V_0^2$$

$$G = \frac{\nu \beta_T g (T_w - T_\infty)}{U_0 V_0^2}, \quad G_C = \frac{\nu \beta_C g (C_w - C_\infty)}{U_0 V_0^2}, \quad (10)$$

where P_r - is the Prandtl number, M - is the magnetic field parameter, G - is the Grashof number, G_C - is the modified Grashof number, S_c - is the Schmidt number and ϕ - is the dimensionless heat absorption coefficient. Furthermore, the spin gradient viscosity γ which gives some relationship between the coefficients of viscosity and micro inertia, is defined as

$$\gamma = \left(\mu + \frac{\wedge}{2} \right) \bar{j} = \mu \bar{j} (1 + 0.5\beta), \quad (11)$$

where β denotes the dimensionless viscosity ratio, defined as follows:

$$\beta = \frac{\wedge}{\mu} \quad (12)$$

in which \wedge is the coefficient of gyro-viscosity. In view of eqs. (8)-(12), the governing eqs. (2)-(5) reduce to the following non-dimensional form:

$$\frac{\partial u}{\partial t} - (1 + \varepsilon A e^{nt}) \frac{\partial u}{\partial y} = \frac{dU_\infty}{dt} + (1 + \beta) \frac{\partial^2 u}{\partial y^2}$$

$$+ G\theta + G_C C + N(U_\infty - u) + 2\beta \frac{\partial \omega}{\partial y}, \quad (13)$$

$$\frac{\partial \omega}{\partial t} - (1 + \varepsilon A e^{nt}) \frac{\partial \omega}{\partial y} = \frac{1}{\eta} \frac{\partial^2 \omega}{\partial y^2}, \quad (14)$$

$$\frac{\partial \theta}{\partial t} - (1 + \varepsilon A e^{nt}) \frac{\partial \theta}{\partial y} = \frac{1}{P_r} \frac{\partial^2 \theta}{\partial y^2} - \phi \theta, \quad (15)$$

$$\frac{\partial C}{\partial t} - (1 + \varepsilon A e^{nt}) \frac{\partial C}{\partial y} = \frac{1}{S_c} \frac{\partial^2 C}{\partial y^2}, \quad (16)$$

$$\text{where, } N = \left(M + \frac{1}{K} \right), \quad \eta = \frac{\mu j}{\gamma} = \frac{2}{2 + \beta}.$$

By setting G_C and ϕ equal to zero and ignoring eq. (16), eqs. (13) and (15) reduce to those reported, by Kim [19]. Also setting β equal to zero and ignoring eq. (14), reduce to those reported by Chamkha [20]. The boundary conditions (6) and (7) are then given by the following dimensionless form:

$$u = U_p, \quad \theta = 1 + \varepsilon e^{nt}, \quad C = 1 + \varepsilon e^{nt},$$

$$\frac{\partial \omega}{\partial y} = -\frac{\partial^2 u}{\partial y^2} \quad \text{at } y = 0, \quad (17)$$

$$u \rightarrow U_\infty, \quad \theta \rightarrow 0, \quad C \rightarrow 0, \quad \omega \rightarrow 0 \quad \text{as } y \rightarrow \infty. \quad (18)$$

3. Solution of the problem

The above system of partial differential equations is to be reduced in dimensionless form, that can be solved analytically. This can be done by representing the linear and angular velocity, temperature and concentration as:

$$u = u_0(y) + \varepsilon e^{nt} u_1(y) + \dots, \quad (19)$$

$$\omega = \omega_0(y) + \varepsilon e^{nt} \omega_1(y) + \dots, \quad (20)$$

$$\theta = \theta_0(y) + \varepsilon e^{nt} \theta_1(y) + \dots, \quad (21)$$

$$C = C_0(y) + \varepsilon e^{nt} C_1(y) + \dots. \quad (22)$$

Substituting eqs (19)-(22) in eqs. (13)-(16), equating the harmonic and non-harmonic terms, and neglecting the coefficient of $O(\varepsilon^2)$, we get the following pairs of equations for $(u_0, \omega_0, \theta_0, C_0)$ and $(u_1, \omega_1, \theta_1, C_1)$.

$$(1 + \beta)u_0'' + u_0' - Nu_0 = -N - G\theta_0 - GC_0 - 2\beta\omega_0', \quad (23)$$

$$(1 + \beta)u_1'' + u_1' - (N + n)u_1 = -(N + n) - \Lambda u_0' - G\theta_1 - GC_1 - 2\beta\omega_1', \quad (24)$$

$$\omega_0'' + \eta\omega_0' = 0, \quad (25)$$

$$\omega_1'' + \eta\omega_1' - n\eta\omega_1 = -\Lambda\eta\omega_0', \quad (26)$$

$$\theta_0'' + Pr\theta_0' = Pr\phi\theta_0, \quad (27)$$

$$\theta_1'' + Pr\theta_1' - (n + \phi)Pr\theta_1 = -AP_r\theta_0', \quad (28)$$

$$C_0'' + ScC_0' = 0, \quad (29)$$

$$C_1'' + ScC_1' - nScC_1 = -AS_C C_0', \quad (30)$$

where a prime denotes differentiation with respect to y . The corresponding boundary conditions can be written as:

$$u_0 = U_p, \quad u_1 = 0, \quad \omega_0' = -u_0'', \quad \omega_1' = -u_1'',$$

$$\theta_0 = 1, \quad \theta_1 = 1, \quad C_0 = 1, \quad C_1 = 1 \quad \text{at } y = 0, \quad (31)$$

$$u_0 = 1, \quad u_1 = 1, \quad \omega_0 \rightarrow 0, \quad \omega_1 \rightarrow 0, \quad \theta_0 \rightarrow 0,$$

$$\theta_1 \rightarrow 0, \quad C_0 \rightarrow 0, \quad C_1 \rightarrow 0 \quad \text{as } y \rightarrow \infty. \quad (32)$$

Without going into detail, the solution, of eqs. (23)-(30), subject to eqs. (31) and (32), can be written as

$$C_0 = e^{-S_C y}, \quad (33)$$

$$C_1 = e^{\lambda_1 y} + \frac{AS_C}{n} \left(e^{\lambda_1 y} - e^{-S_C y} \right), \quad (34)$$

$$\theta_0 = e^{\lambda_2 y}, \quad (35)$$

$$\theta_1 = a_1 e^{\lambda_2 y} + (1 - a_1) e^{\lambda_3 y}, \quad (36)$$

$$\omega_0 = b_1 e^{-\eta y}, \quad (37)$$

$$\omega_1 = b_2 e^{-h_1 y} - \frac{A\eta}{n} b_1 e^{-\eta y}, \quad (38)$$

$$u_0(y) = 1 + d_1 e^{-h_2 y} + a_2 e^{\lambda_2 y} + a_3 e^{-S_C y} + a_4 e^{-\eta y}, \quad (39)$$

$$u_1(y) = 1 + d_2 e^{-h_3 y} + a_5 e^{-h_2 y} + a_6 e^{\lambda_2 y} + a_7 e^{-S_C y} + a_8 e^{-\eta y} + a_9 e^{-\lambda_1 y} + a_{10} e^{-\lambda_1 y} + a_{11} e^{-h_1 y}, \quad (40)$$

Therefore, we obtain the stream wise, angular velocity, temperature and concentration, as follows:

$$u(y, t) = 1 + d_1 e^{-h_2 y} + a_2 e^{\lambda_2 y} + a_3 e^{-S_C y} + a_4 e^{-\eta y} + \varepsilon e^{nt} (1 + d_2 e^{-h_1 y} + a_5 e^{-h_2 y} + a_6 e^{\lambda_2 y} + a_7 e^{-S_C y} + a_8 e^{-\eta y} + a_9 e^{\lambda_1 y} + a_{10} e^{\lambda_1 y} + a_{11} e^{-h_1 y}),$$

$$\omega(y, t) = b_1 e^{-\eta y} + \varepsilon e^{nt} (b_2 e^{-h_1 y} - \frac{A\eta}{n} b_1 e^{-\eta y})$$

$$\theta(y, t) = e^{\lambda_2 y} + \varepsilon e^{nt} ((1 - a_1) e^{\lambda_1 y} + a_1 e^{\lambda_2 y})$$

$$C(y, t) = e^{-S_C y} + \varepsilon e^{nt} (e^{\lambda_1 y} + (e^{\lambda_1 y} - e^{-S_C y}) \frac{AS_C}{n}).$$

Given the velocity field in the boundary layer, the Skin friction coefficient, the Nusselt number and the Sherwood number are important physical parameters for this type of boundary layer flow, which are given by

$$\tau_w = \frac{\partial u}{\partial y} \Big|_{y=0} = -d_1 h_2 + a_2 \lambda_2 - a_3 S_C - a_4 \eta - \varepsilon e^{nt} (d_2 h_3 + a_5 h_2 - a_6 \lambda_2 + a_7 S_C + a_8 \eta - a_9 \lambda_3 - a_{10} \lambda_1 + a_{11} h_1),$$

$$Nu Re_x^{-1} = \frac{\partial \theta}{\partial y} \Big|_{y=0} = \lambda_2 + \varepsilon e^{nt} (\lambda_3 (1 - a_1) + a_1 \lambda_2),$$

$$Sh Re_x^{-1} = \frac{\partial C}{\partial y} \Big|_{y=0} = -S_C + \varepsilon e^{nt} (\lambda_1 + (\lambda_1 + S_C) \frac{AS_C}{n}),$$

where $Re_x = V_0 x/\nu$ is the local Reynolds number.

It should be mentioned that in the absence of concentration buoyancy and heat absorption effects, all of the flow and heat transfer solutions reported above are consistent with those reported earlier by Kim [19]. Also, when $\beta = 0$, and ignoring eq. (14), all the flow and heat transfer solutions reported above are consistent with those reported by Chamkha [20] and therefore will not be repeated here.

Here..

$$\lambda_1 = \frac{-S_c - \sqrt{S_c^2 + 4nS_c}}{2}$$

$$\lambda_2 = \frac{-P_r - \sqrt{P_r^2 + 4P_r\phi}}{2}$$

$$\lambda_3 = \frac{-P_r - \sqrt{P_r^2 + 4(n+\phi)P_r}}{2}$$

$$a_1 = \frac{-AP_r\lambda_2}{\lambda_2^2 + P_r\lambda_2 - (n+\phi)P_r}$$

$$h_1 = \frac{\eta + \sqrt{\eta^2 + 4n\eta}}{2}$$

$$h_2 = \frac{1}{2(1+\beta)}(1 + \sqrt{1 + 4(1+\beta)N})$$

$$a_2 = \frac{-G}{(1+\beta)\lambda_2^2 + \lambda_2 - N}$$

$$a_3 = \frac{-G_c}{(1+\beta)S_c^2 - S_c - N}$$

$$a_4 = \frac{2\beta b_1 \eta}{(1+\beta)\eta^2 - \eta - N}$$

$$d_1 = U_p - 1 - a_2 - a_3 - a_4$$

$$b_1 = \frac{d_1}{\eta} h_2^2 + \frac{a_2}{\eta} \lambda_2^2 + \frac{a_3}{\eta} S_c^2 + a_4 \eta$$

$$h_3 = \frac{1}{2(1+\beta)}(1 + \sqrt{1 + 4(1+\beta)(N+n)})$$

$$a_5 = \frac{\Lambda d_1 h_2}{(1+\beta)h_2^2 - h_2 - (N+n)}$$

$$a_6 = \frac{-(a_2 \lambda_2 A + G a_1)}{(1+\beta)\lambda_2^2 + \lambda_2 - (N+n)}$$

$$a_7 = \frac{(a_3 n + G_c) S_c A}{n((1+\beta)S_c^2 - S_c - (N+n))}$$

$$a_8 = \frac{an\eta A - 2A\eta^2\beta b_1}{n(1+\beta)\eta^2 - \eta - (N+n)}$$

$$a_9 = \frac{-G(1-a_1)}{(1+\beta)\lambda_3^2 + \lambda_3 - (N+n)}$$

$$a_{10} = \frac{-G_c(n + \Lambda S_c)}{n((1+\beta)\lambda_1^2 + \lambda_1 - (N+n))}$$

$$a_{11} = \frac{2\beta b_2 h_1}{(1+\beta)h_1^2 - h_1 - (N+n)}$$

$$d_2 = -1 - a_5 - a_6 - a_7 - a_8 - a_9 - a_{10} - a_{11}$$

$$b_2 = \frac{1}{h_1} \left(\frac{A\eta^2 b_1}{n} + d_2 h_3^2 + a_5 h_2^2 + a_6 \lambda_2^2 + a_7 S_c^2 \right.$$

$$\left. + a_8 \eta^2 + a_9 \lambda_3^2 + a_{10} \lambda_1^2 + a_{11} h_1^2 \right)$$

4. Results and discussions

To study the behavior of the velocity, angular velocity, temperature and concentration profiles, curves are drawn for various values of the parameters that describe the flow. For the case of different values of viscosity ratio β , the velocity and angular velocity profiles are shown in Figures 1, 2. The velocity

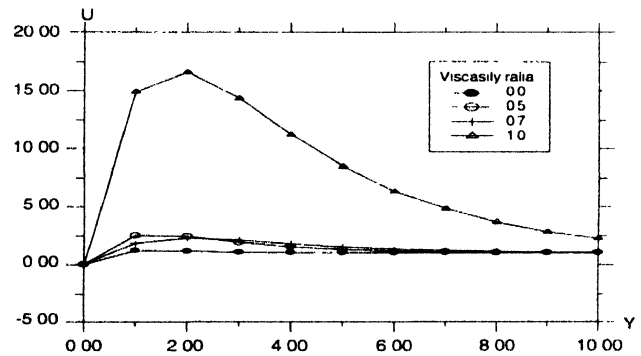


Figure 1. Effects of β on velocity profiles with ($n=0.1, P_r=1.0, A=0.0, U_p=0.0, G=2.0, \epsilon=0.2, t=1.0, M=0, K=0.5, \phi=1.0$)

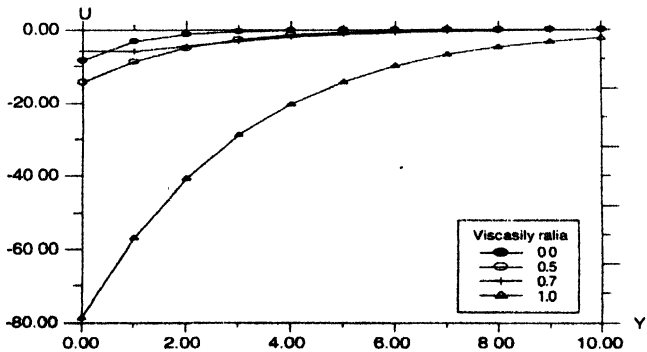


Figure 2. Effects of β on angular velocity profiles with ($n=0.1, P_r=1.0, A=0.0, U_p=0.0, G=2.0, \epsilon=0.2, t=1.0, M=0, K=0.5, \phi=1.0$)

increases with an increase in β , while the angular velocity decreases with an increase in β .

Figures 3-5 illustrate the velocity, temperature and angular velocity profiles respectively, against spanwise coordinate y for different values of dimensionless exponential index n . The results show that increasing values of n , results in an increasing velocity within the boundary layer, which eventually approaches

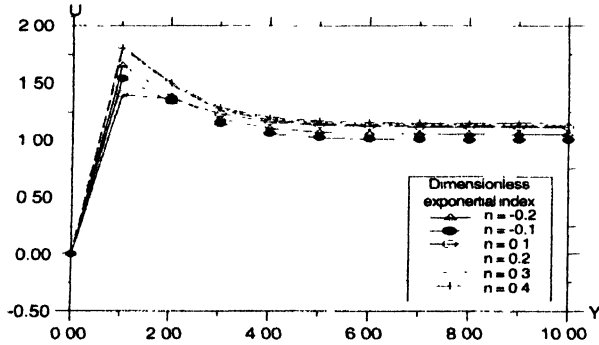


Figure 3. Velocity profiles for different values of dimensionless exponential index n with ($\phi=1.0$, $\beta=0.2$, $P_r=1.0$, $S_c=1.0$, $A=0.5$, $U_p=0.0$, $\epsilon=0.1$, $G=2.0$, $G_c=1.0$, $t=1.0$, $M=2.0$, $K=0.5$).

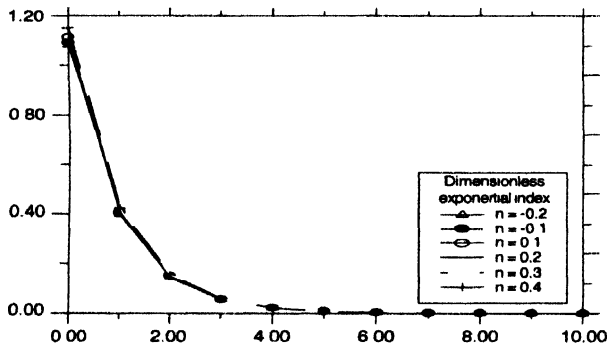


Figure 4. Temperature profiles for different values of dimensionless exponential index n with ($\phi=1.0$, $\beta=0.2$, $P_r=1.0$, $S_c=1.0$, $A=0.5$, $U_p=0.0$, $\epsilon=0.1$, $G=2.0$, $G_c=1.0$, $t=1.0$, $M=2.0$, $K=0.5$).

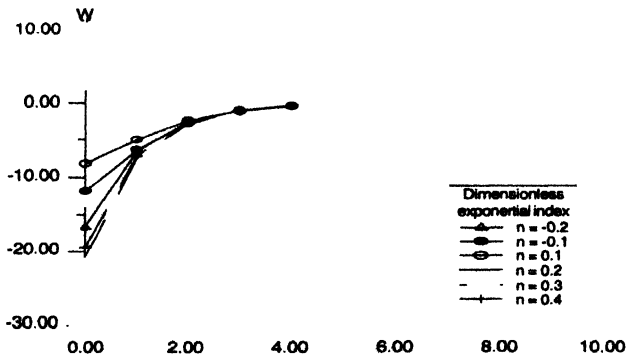


Figure 5. Angular velocity profiles for different values of dimensionless exponential index n with ($\phi=1.0$, $\beta=0.2$, $P_r=1.0$, $S_c=1.0$, $A=0.5$, $U_p=0.0$, $\epsilon=0.1$, $G=2.0$, $G_c=1.0$, $t=1.0$, $M=2.0$, $K=0.5$).

to the relevant free stream velocity at the edge of boundary layer. As the exponential index n increases, the temperature profile increases, while the results show that increasing values of n parameter results in a decreasing angular velocity within the boundary layer, which eventually approaches to the relevant free stream velocity at the edge of boundary layer.

Figures 6, 7 depict the variation of velocity and angular velocity profiles against spanwise coordinate y for different values of plate moving velocity U_p in the direction of fluid flow. The peak value of velocity across the boundary layer decreases near the porous plate as the plate velocity increases, while the values of angular velocity on the porous plate are increased as the plate velocity increases.

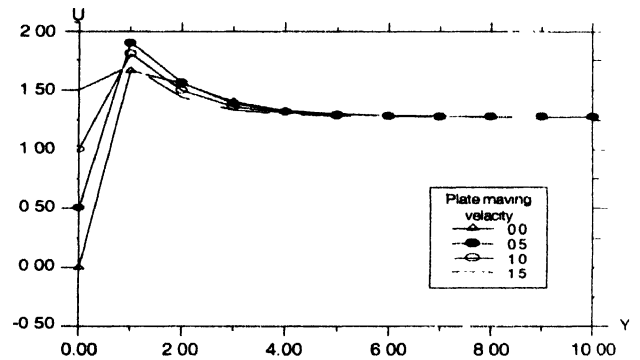


Figure 6. Velocity profiles for different values of plate moving velocity U_p , with ($\phi=1.0$, $\beta=0.2$, $P_r=1.0$, $S_c=1.0$, $A=0.5$, $G=2.0$, $G_c=1.0$, $\epsilon=0.1$, $t=1.0$, $M=2.0$, $K=0.5$).

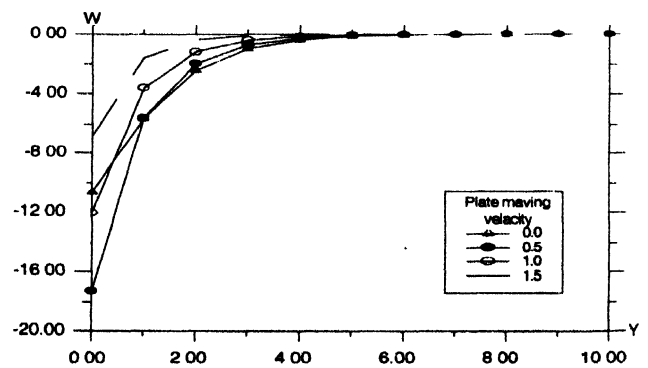


Figure 7. Angular velocity profiles for different values of plate moving velocity U_p , with ($\phi=1.0$, $\beta=0.2$, $P_r=1.0$, $S_c=1.0$, $A=0.5$, $G=2.0$, $G_c=1.0$, $\epsilon=0.1$, $t=1.0$, $M=2.0$, $K=0.5$).

Figures 8, 9 display the effects of magnetic parameter M on velocity and angular velocity profiles respectively. It is obvious that the effect of increasing values of magnetic field parameter results in a decreasing velocity profiles across the boundary layer. Furthermore, the results show that the values of angular velocity on the porous plate are decreased as M increases.

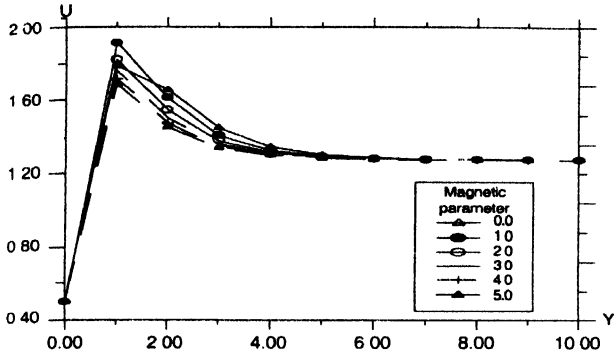


Figure 8. Velocity profiles for different values of magnetic parameter M , with $(\phi=1.0, \beta=0.2, P_r=1.0, S_c=1.0, A=0.5, G=2.0, G_c=1.0, \epsilon=0.1, t=1.0, U_p=0.5, K=0.5)$

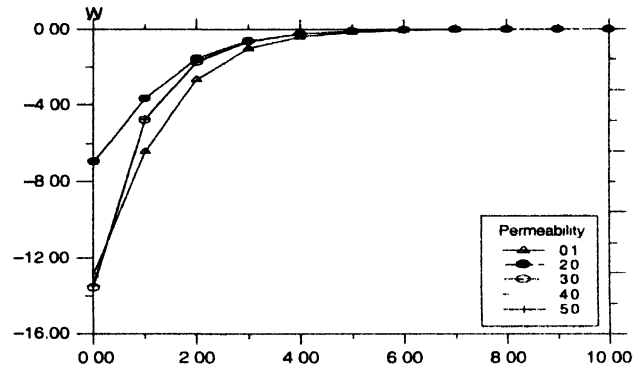


Figure 11. Angular velocity profiles for different values of permeability K , with $(\phi=1.0, \beta=0.2, P_r=1.0, S_c=1.0, A=0.5, G=2.0, G_c=1.0, \epsilon=0.1, t=1.0, U_p=0.5, M=2.0)$

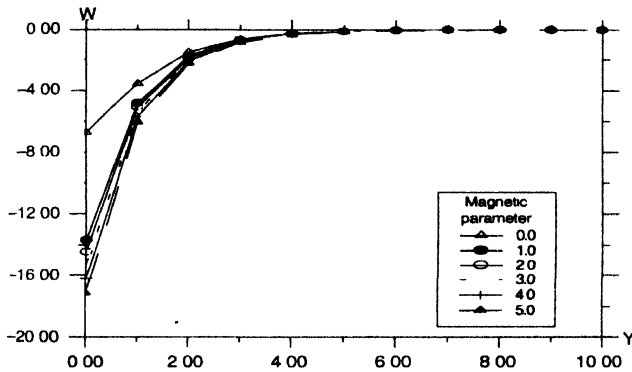


Figure 9. Angular velocity profiles for different values of magnetic parameter M with $(\phi=1.0, \beta=0.2, P_r=1.0, S_c=1.0, A=0.5, G=2.0, G_c=1.0, \epsilon=0.1, t=1.0, U_p=0.5, K=0.5)$

Figures 10, 11 show the velocity and angular velocity profiles against spanwise coordinate y for different values of the permeability parameter K , respectively. Clearly as K increases the velocity boundary layer tends to increase, and then decay to the relevant free stream velocity.

Figures 12 and 13 illustrate the velocity and angular velocity profiles for different values of Grashof number G , respectively. It is shown that an increase in G leads to a rise in the values of velocity but decreases due to angular velocity. Here, the positive value of G corresponds to a cooling of the surface by natural convection. Also, the curves depict that the peak value of

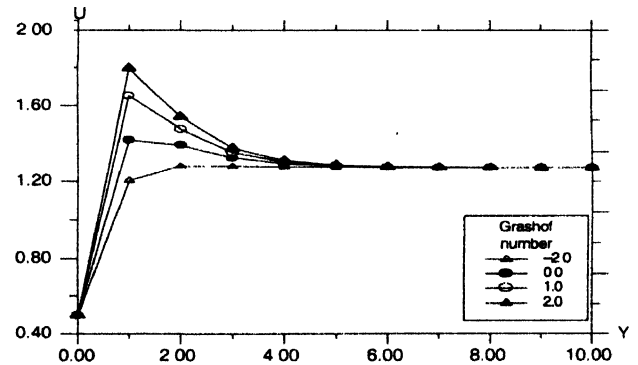


Figure 12. Velocity profiles for different values of Grashof number G , with $(\phi=1.0, \beta=0.2, P_r=1.0, S_c=1.0, A=0.5, K=0.5, G_c=1.0, \epsilon=0.1, t=1.0, U_p=0.5, M=2.0)$

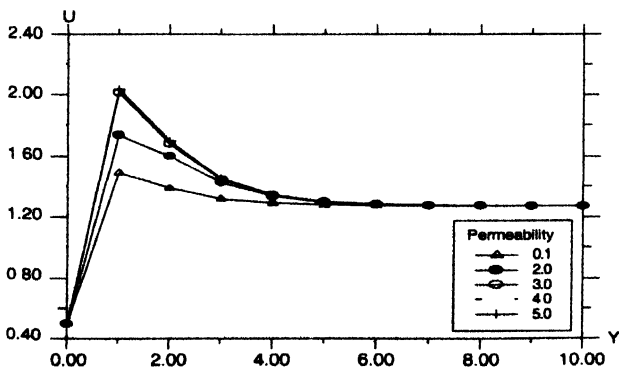


Figure 10. Velocity profiles for different values of permeability K with $(\phi=1.0, \beta=0.2, P_r=1.0, S_c=1.0, A=0.5, G=2.0, G_c=1.0, \epsilon=0.1, t=1.0, U_p=0.5, M=2.0)$

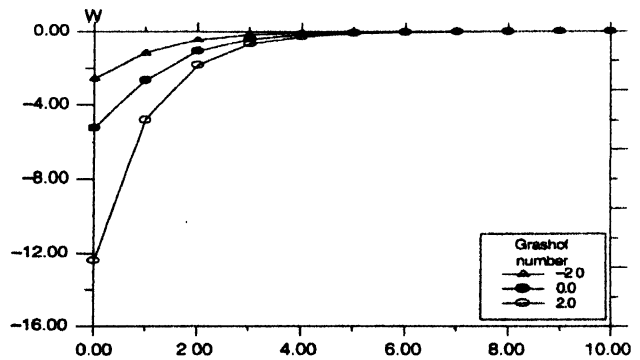


Figure 13. Angular velocity profiles for different values of Grashof number G , with $(\phi=1.0, \beta=0.2, P_r=1.0, S_c=1.0, A=0.5, K=0.5, G_c=1.0, \epsilon=0.1, t=1.0, U_p=0.5, M=2.0)$

Figure 25 displays the distribution of skin friction against the plate moving velocity U_p at different values of suction velocity parameter A . It is seen from this figure that an increase in the value of A leads to a decrease of the skin friction.

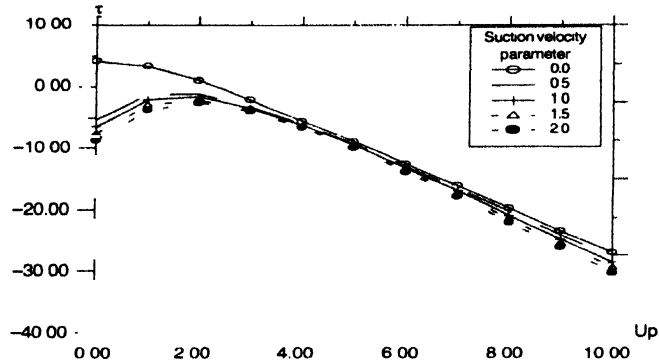


Figure 25. Skin friction profiles for different values of suction velocity parameter with ($\phi=1.0, \beta=0.2, G=2.0, S_c=1.0, P_r=1.0, K=0.5, G_c=1.0, \epsilon=0.1, t=1.0, M=2.0$).

Figure 26 shows the distribution of skin friction against suction velocity parameter A , for various values of Prandtl number. It is seen from this figure that an increase in the value of Prandtl number leads to a decrease of the skin friction coefficient.

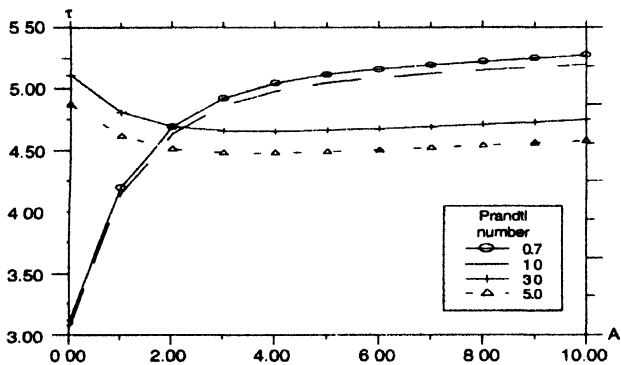


Figure 26. Surface heat transfer profiles for different values of Prandtl number, with ($\phi=1.0, \beta=0.2, G=2.0, S_c=1.0, K=0.5, G_c=1.0, \epsilon=0.1, t=1.0, M=2.0$).

Figure 27 depicts skin friction profiles against suction velocity parameter A , for various values of heat absorption coefficient. This figure shows that an increase in the values of heat absorption coefficient leads to a decrease of the skin friction coefficient.

Figure 28 shows the distribution of skin friction against suction velocity parameter A , for different values of Schmidt number S_c . It is seen that an increase in the value of S_c leads to a decrease of the skin friction.

Figure 29 depicts skin friction profiles against spinwise coordinate y , for different values of modified Grashof number G_c . It is seen from this figure that an increase in the value of G_c leads to an increase of the skin friction.

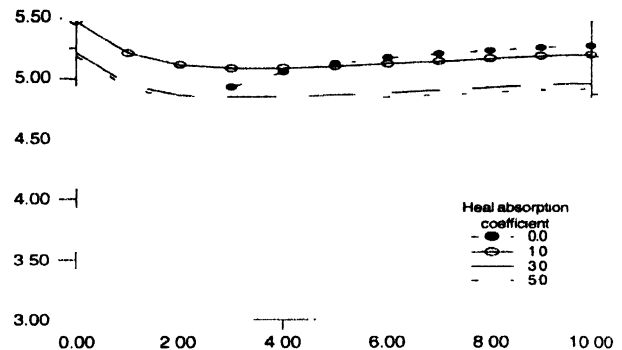


Figure 27. Surface skin friction profiles for different values of heat absorption coefficient, with ($\beta=0.2, G=2.0, S_c=1.0, K=0.5, G_c=1.0, \epsilon=0.1, t=1.0, U_p=0.5, M=2.0, P=1.0, n=1.0$).

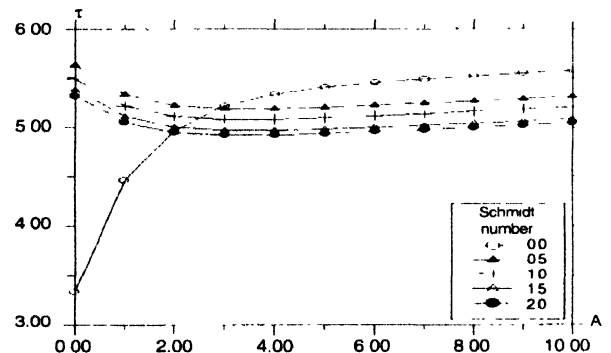


Figure 28. Skin friction profiles for different values of Schmidt number with ($\beta=0.2, G=2.0, K=0.5, \epsilon=0.1, t=1.0, U_p=0.5, M=2.0, P=1.0, A=0.5, n=1.0$).

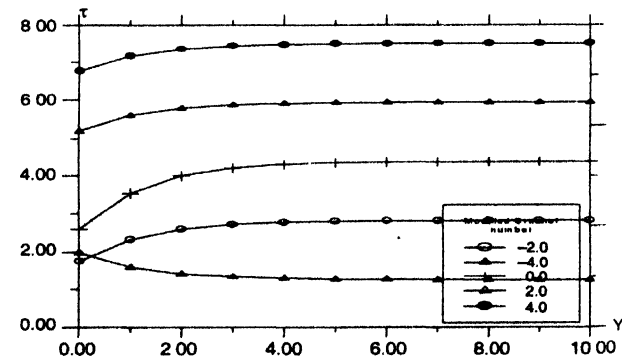


Figure 29. Skin friction coefficient profiles, for different values of modified Grashof number, with ($\beta=0.2, G=2.0, K=0.5, S_c=1.0, \epsilon=0.1, t=1.0, U_p=0.5, M=2.0, A=0.5, n=1.0$).

5. Conclusions

In micropolar fluids, the skin friction coefficient is lower than Newtonian fluids for smaller vortex viscosity parameter, but

higher for larger vortex viscosity parameter. However, the heat transfer rate decreases because of smaller axial velocity for micropolar fluids. Thus, the heat transfer rate of a micropolar fluid is smaller than a Newtonian fluid under all circumstances.

- (i) The velocity increases with an increase in the dimensionless exponential index n , permeability k , Grashof number G and modified Grashof number G_c while it decreases with an increase in plate velocity U_p , magnetic parameter M , Prandtl number Pr , heat absorption ϕ and Schmidt number Sc .
- (ii) The angular velocity increases with an increase in the plate velocity U , permeability K . While it decreases with an increase in dimensionless exponential index n , magnetic parameter m , Grashof number G , Prandtl number Pr , heat absorption, Schmidt number Sc , and modified Grashof number G_c .
- (iii) The concentration decreases with an increase in Schmidt number Sc .
- (iv) The temperature increases with an increase in dimensionless exponential index while decreases with an increase in the Prandtl number Pr and heat absorption coefficient ϕ .
- (v) Skin friction numerically increases with an increase in the modified Grashof number G_c while decreases with an increase in suction velocity parameter A , Prandtl number Pr , Schmidt number Sc and heat absorption ϕ .
- (vi) Sherwood number decreases with an increase in the values of Schmidt number.

The results of the present study are important in practical applications, such as positioning of components dissipating energy on vertical circuit boards embedded in micropolar fluids.

Heat transfer and free convective flow considerations are very important in this area and also in several frequently encountered situations in manufacturing processes.

Acknowledgments

Appreciation is extended to the referees for their constructive and helpful comments and suggestions. These led to improvements in the revised paper.

References

- [1] A C Eringen *Int. J. Engg. Sci.* **2** 205 (1964)
- [2] A C Eringen *J. Math. Mech.* **16** 1 (1966)
- [3] A C Eringen *J. Math. Anal. Appl.* **38** 480 (1972)
- [4] T Arıman and M A Turk and N D Sylvester *Int. J. Engg. Sci.* **11** 905 (1973)
- [5] B C Sakiadis *Am. ICHE J.* **7** 221 (1961)
- [6] T Altan, S Oh and H Gegel *Metal Forming Fundamentals and Applications* (American Society of Metals) (1979)
- [7] E G Fisher *Extrusion of Plastics* (Wiley, New York) (1976)
- [8] Z Tadmor and I Klein *Engineering Principles of Plasticating Extrusion* (Polymer Science) (New York : Van Nostrand Reinhold) (1970)
- [9] M V Karwe and Y Jaluria *J. Heat Transfer* **110** 655 (1988)
- [10] R S R Gorla *Int. J. Engg. Sci.* **26** 385 (1988)
- [11] A A Mohammadein and R S R Gorla *Acta Mechanica* **118** 1 (1996)
- [12] H S Takhar and V M Soundalgekar *Int. J. Engg. Sci.* **23** 201 (1985)
- [13] A A Mohammadein and M A Mansour *Appl. Mech. Engg.* **2** 187 (1997)
- [14] M A El-Hakiem *Appl. Mech. Engg.* **3** 287 (1998)
- [15] M A El-Hakiem *Appl. Mech. Engg.* **4** 509 (1999)
- [16] M A El-Hakiem, A A Mohammadein, S M M El-kabeir and R S R Gorla *Int. Comm. Heat Mass Transfer* **26** 219 (1999)
- [17] T G Cowling *Magneto hydrodynamics* (New York : Inter Science) (1957)
- [18] K Yamamoto and N Iwamura *J. Engg. Math.* **10** 41 (1976)
- [19] J Youn Kim *Inter. J. Engg. Sci.* **38** 833 (2000)
- [20] J Ali Chamkha *Inter. J. Engg. Sci.* **42** 217 (2004)